Journal of Magnetism and Magnetic Materials 399 (2016) 155–158

Contents lists available at ScienceDirect

Journal of Magnetism and Magnetic Materials

journal homepage: www.elsevier.com/locate/jmmm

Stability of topological charge of magnetic skyrmion configurations

M.B.A. Jalil [a,b,*], S.G. Tan [a,b], Z.B. Siu [b,c], W. Gan [d], I. Purnama [d], W.S. Lew [d]

[a] Department of Electrical and Computer Engineering, National University of Singapore, 1 Engineering Drive 3, Singapore
[b] Data Storage Institute, Agency for Science, Technology and Research (A*STAR), DSI Building, 5 Engineering Drive 1, Singapore
[c] NUS Graduate School for Integrative Sciences and Engineering, National University of Singapore, Singapore
[d] School of Physical and Mathematical Sciences, Nanyang Technological University, 21 Nanyang Link, Singapore 637371

ARTICLE INFO

Article history:
Received 8 April 2015
Received in revised form
10 September 2015
Accepted 21 September 2015
Available online 25 September 2015

Keywords:
Skyrmions
Topological charge
Micromagnetics

ABSTRACT

We analyze the topological charge of a skyrmion q_s, and the corresponding Hall conductivity σ_{xy}, which can serve as an electrical read-out for skyrmion-based memory. We derived the general form of the Dzyaloshinskii–Moriya (DM) interaction for any arbitrary orientation of the DM vector $\boldsymbol{D}$. Based on the DM interaction energy, we obtained the dependence the skyrmion helicity angle γ on the orientation of $\boldsymbol{D}$. We showed via general mathematical arguments, the topological nature of the skyrmionic charge q_s, and its independence of γ and specific details of the interior of the skyrmion (e.g., its core size). Finally, we showed via numerical micromagnetics the stability of q_s under varying applied B-fields till the annihilation field, despite the drastic reduction in the skyrmion core size.

Skyrmions, originally introduced as a model for hadrons in nuclear physics [1], are topological objects [2,3] associated with integer invariants, known as their topological charge. Since this invariant is quantized, it is not subject to continuous change due to smooth deformations in the system, thus conferring a high degree of stability to the skyrmion. Skyrmion-like configurations have been observed in magnetic materials, where there are competing interaction terms which result in the canting of the magnetization. In magnetic thin films, the competition between magnetic anisotropy in the perpendicular direction and magnetostatic energy which favours in-plane configuration can lead to the formation of the so-called giant skyrmions [4] of a few hundred microns in size. More recently, smaller magnetic skyrmions of a few tens of nanometers have been observed in various non-centrosymmetric magnets which exhibit the Dzyaloshinskii–Moriya (DM) interaction, which is a type of super-exchange mediated by ions with spin–orbit interaction [5,6]. Such DM-induced skyrmions have been reported in helimagnets such as MnSi [7,8], FeGe [9,10] and $Fe_{1-x}Co_xSi$ [11], and in multiferroic insulators such as Cu_2OSeO_3 [12]. In view of their compact size and robustness conferred by their topological property [13–15], skyrmions have elicited much interest as possible candidates for high-density memory elements. Furthermore, it has been shown that current-induced motion of skyrmions can be induced by current densities as low as $\sim 10^5\ \mathrm{A/m^5}$ [16,17], while controlled writing and annihilation of individual skyrmions via spin injection from a scanning tunneling microscope has also been demonstrated on PdFe bilayer on Ir(111) [18].

Although the presence of skyrmions can be characterized by neutron scattering [8] and Lorentz microscopy [9], for memory application, it would be useful to have an electrical read-out method, especially one which is sensitive to the skyrmion's topological charge q_s. In this paper, we investigate the electrical read-out based on the skyrmionic charge. First, we analyzed the general DM interaction energy of a skyrmion for any arbitrary orientation of the DM vector $\boldsymbol{D}$. Based on the expression for the DM interaction energy and assuming a skyrmion ring model, we obtained the dependence the skyrmion helicity angle γ on the orientation of $\boldsymbol{D}$. Subsequently, we showed by general mathematical arguments, the topological nature of the skyrmionic charge q_s and its independence of the helicity in any parameter space. The topological nature of q_s suggests the stability of any property which is dependent on q_s, such as the Hall conductivity σ_{xy}. We performed exemplary micromagnetic simulation to show the robustness of q_s under a perpendicular B-field, and hence the suitability of utilizing the Hall conductivity σ_{xy} for electrical read-out of skyrmion-based memory.

1. DM energy of skyrmions

First, we consider the different forms of the micromagnetic energy density due to the DM interaction within a two-dimensional magnetic skyrmion configuration as the orientation of the DM vector $\boldsymbol{D}$ varies with respect to the plane of the skyrmion as well as the separation vector between neighbouring moments. If we denote the spatial texture of the skyrmion by $\boldsymbol{n}(\boldsymbol{r})$, then its the

* Corresponding author at: Department of Electrical and Computer Engineering, National University of Singapore, 4 Engineering Drive 3, Singapore 117576

http://dx.doi.org/10.1016/j.jmmm.2015.09.064
0304-8853/

free energy density ε can be written as [19]

$$\varepsilon = \varepsilon_{ex} + \varepsilon_a + \varepsilon_Z + \varepsilon_{DM} = A(\nabla \boldsymbol{n})^2 + K_u(\boldsymbol{n}\cdot\boldsymbol{w}_a)^2 + M_s(\boldsymbol{n}\cdot\boldsymbol{H}_a) + \varepsilon_{DM}, \quad (1)$$

where the first three terms correspond to the usual free energy terms of standard micromagnetics in the continuum limit (namely, the exchange, magnetocrystalline anisotropy and Zeeman energies) [20,21]. Here, A is the exchange stiffness, K_u is the anisotropy constant, $\boldsymbol{w}_a$ is the easy axis direction, $\boldsymbol{H}_a$ is the applied magnetic field and ε_{DM} is the DM interaction energy. The Hamiltonian of the system is then given by the volume integral of ε [2].

To evaluate the form of ε_{DM}, we note that the DM interaction causes canting between neighbouring moments and thus, the discrete DM energy between nearest neighbours i and j can be expressed as $\varepsilon_{DM}^{ij} = \boldsymbol{D}\cdot(\boldsymbol{n}_i \times \boldsymbol{n}_j)$, where the DM vector $\boldsymbol{D}$ sets the axis of spin canting. In terms of spatial derivatives, one can express the interaction energy as

$$\varepsilon_{DM}^{ij} = \boldsymbol{D}\cdot(\boldsymbol{n}_i \times \Delta\boldsymbol{n}_{ij}) = \boldsymbol{D}\cdot[\boldsymbol{n}(\boldsymbol{r}_i) \times (\boldsymbol{r}_{ij}\cdot\nabla)\boldsymbol{n}(\boldsymbol{r}_i)], \quad (2)$$

where $\boldsymbol{r}_{ij}$ is the separation vector. In the case where $\boldsymbol{D}\|\hat{\boldsymbol{r}}_{ij}$, i.e., $\boldsymbol{D} = D_\|\hat{\boldsymbol{r}}_{ij}$, and considering a 2D square lattice with nearest neighbours at $\hat{\boldsymbol{r}}_{ij} = \{\pm a\hat{\boldsymbol{x}}, \pm a\hat{\boldsymbol{y}}\}$, we have

$$\begin{aligned}\varepsilon_{DM}^{\|}(\boldsymbol{r}_i) &\approx D_\| a\left[\hat{\boldsymbol{x}}\cdot\left(\boldsymbol{n} \times \partial_x\boldsymbol{n}\right) + \hat{\boldsymbol{y}}\cdot\left(\boldsymbol{n} \times \partial_y\boldsymbol{n}\right)\right] \\ &= D_\| a(\epsilon_{xqr}n_q\partial_x n_r + \epsilon_{yqr}n_q\partial_y n_r + \epsilon_{zqr}n_q\partial_z n_r) \\ &= D_\| a\epsilon_{pqr}n_q\partial_p n_r = -D_\| a\epsilon_{pqr}n_p\partial_q n_r \\ &= -D_\|'\boldsymbol{n}(\boldsymbol{r}_i)\cdot(\nabla \times \boldsymbol{n}(\boldsymbol{r}_i)),\end{aligned} \quad (3)$$

where in the second line of the above we have added the null (third) term, and $D_\|' = D_\| a$. The approximation in the first line of Eq. (3) holds if the spin texture varies over a length-scale much larger than a. The form of ε_{DM} in Eq. (3) is useful in the continuum limit and is equivalent to the form given in Refs. [22] and [2]. Likewise, we can derive the continuum expression in the case where $\boldsymbol{D}$ is perpendicular to $\boldsymbol{r}_{ij}$ but lying on the plane of atoms, i.e., $\boldsymbol{D}\|(\boldsymbol{r}_{ij} \times \hat{\boldsymbol{z}})$. Summing over the four neighbours as before, we have

$$\begin{aligned}\varepsilon_{DM}^{\perp} &\approx D_\perp a\left[(\hat{\boldsymbol{x}} \times \hat{\boldsymbol{z}})\cdot\left(\boldsymbol{n} \times \partial_x\boldsymbol{n}\right) + (\hat{\boldsymbol{y}} \times \hat{\boldsymbol{z}})\cdot\left(\boldsymbol{n} \times \partial_y\boldsymbol{n}\right)\right] \\ &= D_\perp a\hat{\boldsymbol{z}}\cdot\left[(\boldsymbol{n} \times \partial_i\boldsymbol{n}) \times \hat{\boldsymbol{x}}_i\right] \equiv D_\perp a\hat{\boldsymbol{z}}\cdot\boldsymbol{v},\end{aligned} \quad (4)$$

where $v_j = \varepsilon_{jkl}(\boldsymbol{n} \times \partial_l\boldsymbol{n})_k$. This may be simplified to

$$\begin{aligned}v_j &= \varepsilon_{jkl}(\boldsymbol{n} \times \partial_l\boldsymbol{n})_k = \varepsilon_{jkl}\varepsilon_{kmn}n_m\partial_l n_n = \left(\delta_{lm}\delta_{jn} - \delta_{ln}\delta_{jm}\right)(n_m\partial_l n_n) \\ &= n_l\partial_l n_j - n_j\partial_l n_l\end{aligned}$$

$$\Rightarrow \boldsymbol{v} = [(\boldsymbol{n}\cdot\nabla)\boldsymbol{n}] - \boldsymbol{n}(\nabla\cdot\boldsymbol{n}), \quad (5)$$

and so the DM energy in continuum form for the case of perpendicular DM vector is given by

$$\varepsilon_{DM}^{\perp} = D_\perp'[(\boldsymbol{n}\cdot\nabla)n_z] - n_z(\nabla\cdot\boldsymbol{n}), \quad (6)$$

where $D_\perp' = D_\perp a$.

2. Helicity of skyrmions

The helicity of a skyrmion describes the clockwise or anticlockwise twist of the magnetization orientation within the skyrmion about its core, and is characterized by the helicity angle γ [2,23,24]. Based on the DM energetics discussed in the previous section, we can derive the equilibrium skyrmion configuration and, hence its helicity under varying orientation of the DM vector $\boldsymbol{D}$. We first express the unit vector $\boldsymbol{n}$ along the magnetization direction (which denotes the spin texture of the skyrmion) in terms of the polar and azimuthal spin angles, i.e.,

$$\boldsymbol{n} = (\sin\theta(\boldsymbol{r})\cos\phi(\boldsymbol{r}), \sin\theta(\boldsymbol{r})\sin\phi(\boldsymbol{r}), \cos\theta(\boldsymbol{r})). \quad (7)$$

Due to the rotational symmetry of a general skyrmion configuration, the spin angles θ and ϕ are functions of r and φ only, i.e., $\theta(\boldsymbol{r}) = \theta(r)$ and $\phi(\boldsymbol{r}) = \phi(\varphi)$, where (r, φ) are the spatial cylindrical coordinates. In addition, the polar angle can be any smooth function which obeys the following boundary conditions:

$$\theta(r) = \begin{cases}(P-1)\dfrac{\pi}{2}, & r = 0, \\ (P+1)\dfrac{\pi}{2}, & r \to \infty,\end{cases} \quad (8)$$

where $P = \pm 1$ is the polarity, while the general form for the azimuthal spin angle is $\phi(\varphi) = W\varphi + \gamma$, where W is an integer signifying the winding number, and γ is the helicity angle. In this paper, we will limit the discussion to skyrmions of unit winding number. For the special helicity angles of γ=0 and $\gamma = \pi/2$, the skyrmion adopts the (outward) radial and (counter-clockwise) vortex forms, respectively, which can be mapped to the regular *hedgehog* or *combed hedgehog* on the unit Bloch sphere in spin space [25].

We consider the DM interaction energy between a moment at the centre of a skyrmion and a circular ring of neighbouring moments situated at δr away in the radial direction. For simplicity, we consider polarity P=1, i.e., the polar angle at the centre is $\theta = 0$, while that of the neighbours is $\delta\theta = (\partial_r\theta)\delta r$. Therefore, the change in the moment orientation over $(\delta r)\hat{\boldsymbol{r}}$ is $\Delta\boldsymbol{n} = (\cos\phi, \sin\phi, 0)(\partial_r\theta)\delta r$. Now, suppose the DM vector is aligned within the plane of the moments but at some angle ϑ to the separation direction $\hat{\boldsymbol{r}}$, i.e., $\boldsymbol{D} = D(\cos(\varphi + \vartheta), \sin(\varphi + \vartheta), 0)$. Thus, following Eq. (2) and summing over the ring of neighbours, the total DM interaction energy is given by

$$\begin{aligned}\varepsilon_{DM} \sim \int\boldsymbol{D}\cdot(\boldsymbol{n} \times \Delta\boldsymbol{n})\,d\varphi &= D(\partial_r\theta)\delta r\int_0^{2\pi}\sin(\varphi + \vartheta - \phi(\varphi))\,d\varphi \\ &= -D(\partial_r\theta)\delta r\int_0^{2\pi}\sin[(W-1)\varphi + \gamma \\ &\quad - \vartheta]\,d\varphi.\end{aligned} \quad (9)$$

Supposing $D > 0$ and W=1, the DM energy is thus minimized when $\gamma = \vartheta + \pi/2$. Thus, when $\boldsymbol{D}\|\hat{\boldsymbol{r}}$, i.e., $\vartheta = 0$, we have $\gamma = \pi/2$, which corresponds to the counter-clockwise vortex skyrmion. Conversely, for $\boldsymbol{D}\perp\hat{\boldsymbol{r}}$, i.e., $\vartheta = \pi/2$, $\gamma = \pi$, which corresponds to the inward radial skyrmion. For $D < 0$, the direction and sense of rotation of the skyrmions are reversed. Finally, if $\boldsymbol{D}$ is at some oblique angle to $\hat{\boldsymbol{r}}$, then the resulting skyrmion would have intermediate degree of helicity with $0 < \gamma < \pi/2$. The dependence of the skyrmion helicity to the direction of $\boldsymbol{D}$ is depicted in Fig. 1.

3. Skyrmionic charge and Hall conductivity

It has been shown both theoretically [15,26] and experimentally [27,28] that an electron which traverses through a 2D skyrmionic texture (on the xy plane) and relaxes to the local magnetization direction $\boldsymbol{n}(\boldsymbol{r})$ would experience an *emergent* out-of-plane magnetic field:

$$B_t^z = \frac{\Phi_0}{S}\int\boldsymbol{n}\cdot\left(\partial_x\boldsymbol{n} \times \partial_y\boldsymbol{n}\right)dx\,dy \equiv 4\pi\left(\frac{\Phi_0}{S}\right)q_s, \quad (10)$$

where $\Phi_0 = \hbar/2e$ is the flux quantum, S is the area of the skyrmion and q_s is the skyrmionic charge. The emergent field causes a transverse deflection of electrons, resulting in an additional contribution to the Hall conductivity σ_{xy} over and above the normal Hall (due to applied B-field) and anomalous Hall (due to the net

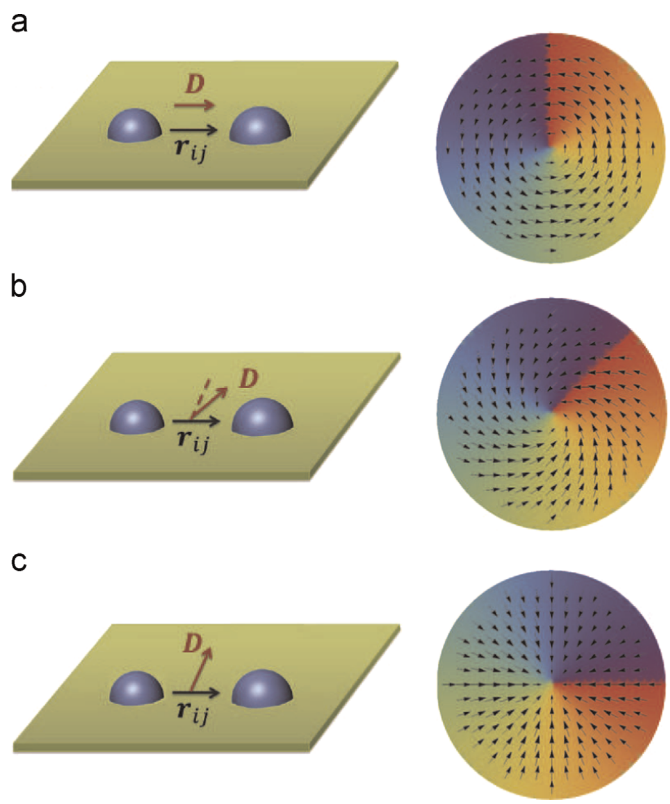

Fig. 1. Dependence of the helicity of the skyrmion configurations on the direction of DM vector $\boldsymbol{D}$ relative to the neighbour separation $\boldsymbol{r}_{ij}$. (a), (b) and (c) correspond to angles $\vartheta = 0, \pi/4, \pi/2$, between $\boldsymbol{D}$ and $\boldsymbol{r}_{ij}$, which yield the helicity angles $\gamma = \pi/2, 3\pi/4, \pi$, respectively.

perpendicular magnetization) contributions. By balancing the resulting Lorentz force due to B_t^z and electrical force due to the transverse E-field, it can be shown that $\sigma_{xy} = \sigma_{xx}(e\tau/m_e)PB_t^z$ [15], where P is the spin polarization of the conduction electron (noting that the topological field has opposite signs for electrons whose spins are anti-aligned to the local moments). Equivalently, we have a proportional relation between the Hall resistivity and the topological field, i.e.,

$$\rho_{xy} \approx \sigma_{xy}/\sigma_{xx}^2 = PB_t^z/ne = PR_H B_t^z, \tag{11}$$

where $R_H = 1/ne$ is the Hall constant. Thus, Hall conductivity/resistivity measurement $\rho_{xy} \propto q_s$ can serve as the read-out of the topological state of skyrmion-based memory elements.

The skyrmionic charge q_s as defined in Eq. (10) is thus an important parameter for an electrical read-out of a skyrmion memory state based on the topological Hall resistivity. We shall now show on general mathematical grounds that q_s, and hence the topological field B_t^z and Hall resistivity ρ_{xy} are *independent* of the helicity angle γ. First, we transform the integrand in Eq. (10) to an arbitrary 2D space characterized by coordinates p and q, as follows:

$$\begin{aligned}\boldsymbol{n}\cdot\left(\partial_x\boldsymbol{n} \times \partial_y\boldsymbol{n}\right) dx\, dy &= \boldsymbol{n}\cdot\left(\partial_p\boldsymbol{n} \times \partial_q\boldsymbol{n}\right)\left[\frac{\partial(p, q)}{\partial(x, y)}\right] dx\, dy \\ &= \boldsymbol{n}\cdot\left(\partial_p\boldsymbol{n} \times \partial_q\boldsymbol{n}\right) dp\, dq,\end{aligned} \tag{12}$$

where the term in the square brackets denotes the Jacobian of the transformation. By choosing $(p, q) = (r, \varphi)$, i.e., the spatial cylindrical coordinates, one obtains $\boldsymbol{n}\cdot(\partial_x\boldsymbol{n} \times \partial_y\boldsymbol{n})\, dx\, dy = \boldsymbol{n}\cdot(\partial_r\boldsymbol{n} \times \partial_\varphi\boldsymbol{n})\, dr\, d\varphi$. Considering the general function representing a skyrmion texture [i.e., $\theta(\boldsymbol{r}) = \theta(r)$, $\phi(\boldsymbol{r}) = W\varphi + \gamma$], we have

$$\left(\partial_r\boldsymbol{n} \times \partial_\varphi\boldsymbol{n}\right) = (\partial_\theta\boldsymbol{n} \times \partial_\phi\boldsymbol{n})\left(\frac{\partial\theta}{\partial r}\right)\left(\frac{\partial\phi}{\partial\varphi}\right) = W\boldsymbol{n}\sin\theta\left(\frac{\partial\theta}{\partial r}\right), \tag{13}$$

where the last equality follows from Eq. (7). By substituting the results in Eqs. (12) and (13) into the definition of the skyrmionic charge in Eq. (10), we thus have

$$\begin{aligned}q_s &= \frac{1}{4\pi}\int \boldsymbol{n}\cdot\left(\partial_x\boldsymbol{n} \times \partial_y\boldsymbol{n}\right) dx\, dy = \frac{1}{4\pi}\int \boldsymbol{n}\cdot\left(\partial_r\boldsymbol{n} \times \partial_\varphi\boldsymbol{n}\right) dr\, d\varphi \\ &= \frac{W}{4\pi}\int (\boldsymbol{n}\cdot\boldsymbol{n})\sin\theta\left(\frac{\partial\theta}{\partial r}\right) dr\, d\varphi = -\frac{W}{2}\int_0^R\left(\frac{\partial}{\partial r}\cos\theta\right) dr \\ &= \frac{W}{2}\left[\cos\theta(0) - \cos\theta(R)\right] = \frac{W}{2}\left[1 - \cos\theta(R)\right],\end{aligned} \tag{14}$$

where R is the radius of the skyrmionic element. Thus, for an ideal skyrmion, its charge q_s is independent of the helicity factor γ. q_s also depends only on the polar angle at the boundaries $r=0$ and $r=R$, and is independent of the specific skyrmion texture within the element itself. This universality hints at the topological nature of q_s. To illustrate this further, one can choose $(p, q) = (\theta, \varphi)$ in Eq. (12), i.e., the coordinates defining the surface of the unit sphere in spin space. In this case,

$$\boldsymbol{n}\cdot\left(\partial_x\boldsymbol{n} \times \partial_y\boldsymbol{n}\right) = \boldsymbol{n}\cdot\left(\partial_\theta\boldsymbol{n} \times \partial_\phi\boldsymbol{n}\right) d\theta\, d\phi = \sin\theta\, d\theta\, d\phi = d\Omega_s, \tag{15}$$

which is none other than the differential solid angle in spin space. Thus, integrating over (θ, ϕ), one finds that $4\pi q_s = \int d\Omega_s = \Omega_s$, which is the solid angle subtended by the skyrmion texture in spin space. For an ideal skyrmion of infinite extent, i.e., $R \to \infty$, $\Omega_s = W$, the winding number, i.e., the number of times the texture *winds* around the unit Bloch sphere. Hence, the Hall resistivity due to the skyrmionic texture $\rho_{xy} \propto \Omega_s = W$ is related to a quantized topological invariant W, and thus resistant to small fluctuations.

As mentioned earlier, the skyrmionic charge q_s and hence the Hall read-out σ_{xy} are only dependent on the magnetization at the centre $(r = 0)$ and at the element boundary $(r = R)$, and independent of the specific skyrmion configuration (e.g., its core size and helicity) in the interior of the element. In other words, q_s and σ_{xy} are the same for any function $\theta(r)$, as long as it varies smoothly with r and obeys the boundary conditions $\theta=0$, and $\theta(R)$ at the centre and edge, respectively. This can be seen analytically by considering the corresponding magnetic vector potential of the topological field B_t, which is given by $\boldsymbol{A}_t(\boldsymbol{r}) = (\Phi_0/2S)(1 - \cos\theta(\boldsymbol{r}))\nabla\phi$, [15]. By applying Stoke's theorem, Eq. (10) simplifies to a line integral around the element boundary: $\oint \boldsymbol{A}_t\cdot d\boldsymbol{r} = (\Phi_0/2S)[1 - \cos\theta(R)]\oint d\phi = (\pi W\Phi_0/S)[1 - \cos\theta(R)]$, which is consistent with Eq. (14).

4. Micromagnetic simulation of q_s

Based on the analysis of the previous section, we find that q_s and hence, any read-out based on it, would be highly robust as long as we can pin the magnetization at the centre and boundary of the skyrmion element. For a numerical test of the robustness of q_s, we perform micromagnetic simulation on a skyrmionic disk element under an applied B-field in the perpendicular (z) direction, and opposite to the magnetization of the skyrmion core. In this set-up, the skyrmion boundary which is magnetized along the field direction would be stabilized by Zeeman interaction, while the magnetization of the skyrmion core is stabilized by the large exchange field required to reverse it. The micromagnetic simulation is performed over a range of applied field strength up to the annihilation field of the skyrmion, i.e., the field strength at which the core is switched to yield a uniform domain along the field direction. We show that despite the drastic reduction in the skyrmion core radius a as the B-field is increased, the corresponding charge q_s remains stable until close to the annihilation field of the skyrmion.

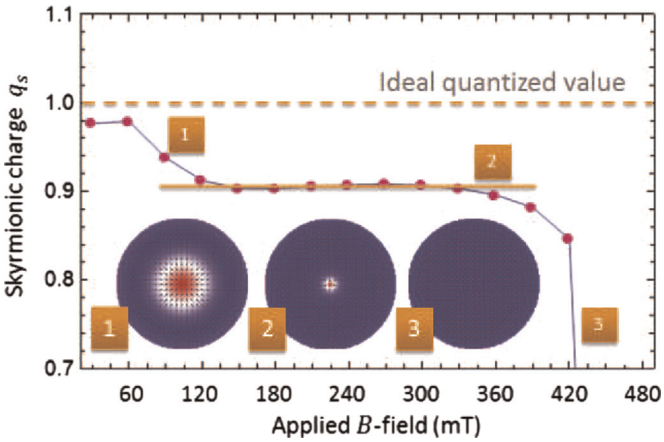

Fig. 2. (Main) Calculated skyrmionic charge q_s of steady state skyrmion configurations under different B-field. Labels 1, 2 and 3 refer to three different field strengths of 90, 360 and 450 mT, respectively. The insets show the configurations at the three field values. Red (blue) regions denote magnetization in the $+z$ $(-z)$ directions. (For interpretation of the references to colour in this figure caption, the reader is referred to the web version of this paper.)

The micromagnetic simulation was performed based on the OOMMF code [29], modified to include the DM interaction [30]. We assume typical magnetic parameters: $D = 1.2\ \mathrm{mJ/m^2}$, $K_u = 370\ \mathrm{kJ/m^3}$, $A = 9 \times 10^{-12}\ \mathrm{J/m}$, and $M_s = 800\ \mathrm{kA/m}$, and consider elements of 50 nm in radius and 1 nm in thickness. The initial magnetization is set to the skyrmion configuration described by $\cos\theta(r) = (a^2 - r^2)/(a^2 + r^2)$, and $\gamma = 0$ (i.e., radial skyrmion), and then relaxed under a uniform field applied in the $-z$ direction. The field strength is varied from 0 to 450 mT. At each field value, the charge q_s as defined in Eq. (10) is numerically calculated based on the steady state configuration $\boldsymbol{n}(\boldsymbol{r})$. As can be seen from the insets of Fig. 2, the skyrmion radius is much reduced in size as the B-field value is increased to 360 mT, before disappearing (annihilation) at 450 mT. However, the value of q_s remains relatively stable and close to the ideal value of unity ($q_s \approx 0.9$) over a wide range of field strength. There is a small reduction in q_s from 1.0 to about 0.9 when the B-field is increased between 60 and 120 mT, due to a slight canting of spins close to the centre. However, as the field is increased further up to 360 mT, the overall skyrmion configuration and hence q_s hold stable even though the core radius undergoes a drastic reduction by a factor of around 5. It is only when the skyrmion is finally switched to the topologically trivial uniform domain at $B = 450$ mT that q_s drops sharply to 0.

By assuming an ideal skyrmion configuration one can obtain the corresponding fields associated with the energy terms in Eq. (1), namely the exchange, anisotropy and DM fields (in the z-direction and taken at the skyrmion centre):

$$\boldsymbol{H}^z_{ex} = \frac{2A}{\mu_0 M_s}\Delta n_z = \frac{16A}{\mu_0 M_s a^2},$$
$$\boldsymbol{H}^z_{K,eff} = \frac{2K_u}{\mu_0 M_s} - N_z M_s,$$
$$\boldsymbol{H}^z_{DM} = \frac{D}{\mu_0 M_s}\left(\frac{2a}{a^2 + r^2}\right) = \frac{2D}{\mu_0 M_s a}, \tag{16}$$

where the demagnetizing factor can be taken to be $N_z \approx 1$ for a thin disk. Assuming $a \approx 7.5$ nm, which correspond to the critical radius $\sim A_{ex}/D$, the numerical field values are $\boldsymbol{B}^z_{ex} \approx 0.4$ T, $\boldsymbol{B}^z_K \approx -0.08$ T, and $\boldsymbol{B}^z_{DM} \approx 0.2$ T. Thus, the required field to overcome these fields and switch (annihilate) the skyrmion core is ≈0.5 T, which is reasonably close to the numerical value of 420 mT. The relative stiffness of the skyrmion core up to a relatively large field value would ensure the skyrmionic read-out via Hall conductivity to be robust and undisturbed by stray fields.

In summary, we have analyzed the DM interaction energy of a skyrmion for varying orientation of the DM vector $\boldsymbol{D}$. Based on the DM interaction and assuming a skyrmion model consisting of a ring of neighbouring moments, we showed the relation between the orientation of $\boldsymbol{D}$ and the skyrmion helicity angle γ. We then show the topological nature of the skyrmionic charge q_s and its independence of the helicity via general mathematical arguments. The topological nature of q_s suggests the stability of any property which is dependent on q_s, such as the Hall conductivity σ_{xy}. We show via an exemplary micromagnetic simulation the robustness of q_s under a perpendicular B-field, and hence the suitability of utilizing the Hall conductivity σ_{xy} for the read-out of skyrmion-based memory.

Acknowledgements

We thank the National Research Foundation of Singapore under the Competitive Research Programs “Non-Volatile Magnetic Logic and Memory Integrated Circuit Devices” NRF-CRP9-2011-01 and “Next Generation Spin Torque Memories: from Fundamental Physics to Applications” NRF-CRP9-2013-01 for financial support.

References

[1] T.H.R. Skyrme, Proc. R. Soc. A 260 (1961) 127.
[2] N. Nagaosa, Y. Tokura, Nat. Nanotechnol. 8 (2013) 899.
[3] L. Ye-Hua, L. You-Quan, Chin. Phys. B 24 (2015) 17506.
[4] M. Ezawa, Phys. Rev. Lett. 105 (2010) 197202.
[5] I. Dzyaloshinsky, J. Phys. Chem. Solids 4 (1958) 241.
[6] T. Moriya, Phys. Rev. 120 (1960) 91.
[7] Y. Ishikawa, K. Tajima, D. Bloch, M. Roth, Solid State Commun. 19 (1976) 525.
[8] S. Mühlbauer, et al., Science 323 (2009) 915.
[9] X. Yu, et al., Nat. Mater. 10 (2011) 106.
[10] S. Huang, C. Chien, Phys. Rev. Lett. 108 (2012) 267201.
[11] X. Yu, Y. Onose, N. Kanazawa, J. Park, J. Han, Y. Matsui, N. Nagaosa, Y. Tokura, Nature 465 (2010) 901.
[12] S. Seki, X. Yu, S. Ishiwata, Y. Tokura, Science 336 (2012) 198.
[13] J. Sampaio, V. Cros, S. Rohart, A. Thiaville, A. Fert, Nat. Nanotechnol. 8 (2013) 839.
[14] M.B.A. Jalil, S.G. Tan, K. Eason, J.F. Kong, J. Appl. Phys. 115 (2014) 17D107.
[15] M.B.A. Jalil, S.G. Tan, Sci. Rep. 4 (2014) 5123.
[16] X. Yu, et al., Nat. Commun. 3 (2012) 988.
[17] J. Iwasaki, M. Mochizuki, N. Nagaosa, Nat. Commun. 4 (2013) 1463.
[18] N. Romming, et al., Science 341 (2013) 636.
[19] J.H. Han, J. Zang, Z. Yang, J.-H. Park, N. Nagaosa, Phys. Rev. B 82 (2010) 094429.
[20] A. Aharoni, Introduction to the Theory of Ferromagnetism, vol. 109, Oxford University Press, Oxford, 2000, p. 174ff.
[21] J.M. Coey, Magnetism and Magnetic Materials, Cambridge University Press, Cambridge, 2010, p. 231ff.
[22] K. Everschor, M. Garst, B. Binz, F. Jonietz, S. Mühlbauer, C. Pfleiderer, A. Rosch, Phys. Rev. B 86 (2012) 054432.
[23] D. Morikawa, K. Shibata, N. Kanazawa, X. Yu, Y. Tokura, Phys. Rev. B 88 (2013) 024408.
[24] X. Zhang, M. Ezawa, Y. Zhou, Sci. Rep. 5 (2015) 9400.
[25] K. Everschor, Current-induced dynamics of chiral magnetic structures (Thesis).
[26] G. Tatara, H. Kohno, J. Shibata, Y. Lemaho, K.-J. Lee, J. Phys. Soc. Jpn. 76 (2007) 054707.
[27] A. Neubauer, C. Pfleiderer, B. Binz, A. Rosch, R. Ritz, P.G. Niklowitz, P. Böni, Phys. Rev. Lett. 102 (2009) 186602.
[28] T. Schulz, et al., Nat. Phys. 8 (2012) 301.
[29] M. Donahue, D. Porter, Object Oriented Micromagnetic Framework, see ⟨http://math.nist.gov/oommf/⟩.
[30] S. Rohart, X. Zhang, ⟨https://www.lps.u-psud.fr/spip.php?article2252⟩.